CHEMISTRY

A polyaromatic receptor with high androgen affinity

Masahiro Yamashina*, Takahiro Tsutsui, Yoshihisa Sei, Munetaka Akita, Michito Yoshizawa†

Biological receptors distinguish and bind steroid sex hormones, e.g., androgen-, progestogen-, and estrogen-type hormones, with high selectivity. To date, artificial molecular receptors have been unable to discriminate between these classes of biosubstrates. Here, we report that an artificial polyaromatic receptor preferentially binds a single molecule of androgenic hormones, known as "male" hormones (indicated with *m*), over progestogens and estrogens, known as "female" hormones (indicated with *f*), in water. Competitive experiments established the binding selectivity of the synthetic receptor for various sex hormones to be testosterone (*m*) > androsterone (*m*) >> progesterone (*f*) > β-estradiol (*f*) > pregnenolone (*f*) > estriol (*f*). These bindings are driven by the hydrophobic effect, and the observed selectivity arises from multiple CH-π contacts and hydrogen-bonding interactions in the semirigid polyaromatic cavity. Furthermore, micromolar fluorescence detection of androgen was demonstrated using the receptor containing a fluorescent dye in water.

INTRODUCTION

The selective binding and sequestration of substrates by protein pockets is the decisive step for a wide range of biological recognition and enzyme catalysis. The imitation of this step by synthetic molecular receptors has long been heralded as necessary for the development of ultrasensitive analytical devices based on single-molecule detection (*1*–*3*). Steroid sex hormones are particularly attractive substrate targets with a polycyclic skeleton (Fig. 1A), as these molecules are essential and highly active biosignals in vertebrate animals (*4*). On the basis of their biological functions, the hormones are divided into three broad classes: androgen, progestogen, and estrogen. The corresponding bioreceptors (30 to 110 kDa in molecular mass) recognize and bind the substrates with high specificity in water (*4*, *5*). For example, androgenic hormones such as testosterone and androsterone, known as "male" hormones, are selectively and tightly bound by the protein pocket of a human androgen receptor (Fig. 1B, left) (*6*, *7*). The binding affinities for progestogens and estrogens, known as "female" hormones, are much lower (*8*). The steroid structures are quite similar, featuring a relatively rigid tetracyclic framework with different small functional groups on the terminal A and D rings (Fig. 1A), so that the selective recognition remains a substantial challenge. There are several reports on synthetic receptors that exhibit high binding abilities for specific sex hormones and derivatives in organic solvents and water (*9*–*21*). In addition, their fluorescent detection has been demonstrated with high sensitivity (*10*, *11*, *17*). However, artificial receptors that can strictly distinguish between male and female hormones from the mixtures, such as biological androgen receptors, remain unreported (*22*, *23*).

Here, we report that capsule-shaped molecular receptor **1** (Fig. 1C) binds a single molecule of androgenic hormones in the cavity with high affinity (K_a = ~10^7 M^{-1}) in water. Competitive experiments reveal that the synthetic receptor preferentially binds various natural sex hormones in a fashion similar to biological androgen receptors: androgens [e.g., testosterone (**2a**) and androsterone] >> progestogens and estrogens [e.g., progesterone (**3a**), β-estradiol (**4a**), and estriol] (Fig. 1D and fig. S1). The x-ray crystallographic analysis of the resultant host-guest complex suggests that the observed selectivity arises from multiple CH/OH-π and hydrogen-bonding interactions between the substrates and the polyaromatic frameworks of **1**. We also report the fluorescence detection of testosterone binding in water on the nanogram scale using an indicator displacement assay.

The earliest artificial receptors provide cage-shaped and tubular frameworks, mainly composed of aliphatic subunits (e.g., glucoses and glycolurils) (*9*, *10*) with an occasional small aromatic ring (e.g., benzene and naphthalene rings) (*12*–*16*). The cavities are generally open or partially enclosed by covalently linked organic frameworks, except for a self-assembled cavitand-based capsule (*18*). Molecular receptor **1** (*24*), on the other hand, is constructed of polyaromatic anthracene panels (Fig. 1C, left) and offers an isolated cavity capable of effective hydrophobic π-π and CH-π interactions (*25*–*27*) with aromatic and aliphatic substrates, respectively (*24*, *28*–*34*). The cavity is fully encircled by four bent polyaromatic ligands linked by two Pt(II) ions (Fig. 1C, right). The metal-ligand bonds allow the receptor to behave as a semirigid spherical container with an inner diameter of ~1 nm and a changeable cavity volume of 430 to 690 $Å^3$ (*35*). The dimensions are slightly larger than those of male and female hormones (290 to 360 $Å^3$ in molecular volume and 1.1 to 1.4 nm in long axis). Besides its smaller and more robust structure (Fig. 1B, right) in comparison with the biological receptors (e.g., Fig. 1B, left), the above characteristic properties of aqueous synthetic receptor **1** prompted us to explore its discriminative ability between male and female hormones.

RESULTS

Selective binding of testosterone from mixtures

Synthetic receptor **1** quantitatively binds a single molecule of representative male hormone, i.e., testosterone (**2a**), and female hormones, i.e., progesterone (**3a**) and β-estradiol (**4a**), but shows a distinct binding preference for the male over the female hormones in water (Fig. 2A). When a mixture of hydrophobic hormones **2a**, **3a**, and **4a** (0.39 μmol each) was suspended in a D_2O solution (0.5 ml) of receptor **1** (0.39 μmol; Fig. 2B) at 60°C for 10 min, the receptor predominantly bound a single molecule of **2a** in the hydrophobic cavity of **1** to give 1:1 host-guest complex **1**•**2a** in >98% yield (Fig. 2C and figs. S2 to S4), confirmed by the ^{1}H nuclear magnetic resonance (NMR) analysis. To fully characterize the product structure, we separately prepared complex **1**•**2a** under the same conditions without

Laboratory for Chemistry and Life Science, Institute of Innovative Research, Tokyo Institute of Technology, 4259 Nagatsuta, Midori-ku, Yokohama 226-8503, Japan.
*Present address: Department of Chemistry, School of Science, Tokyo Institute of Technology, 2-12-1 Ookayama, Meguro-ku, Tokyo 152–8551, Japan.
†Corresponding author. Email: yoshizawa.m.ac@m.titech.ac.jp

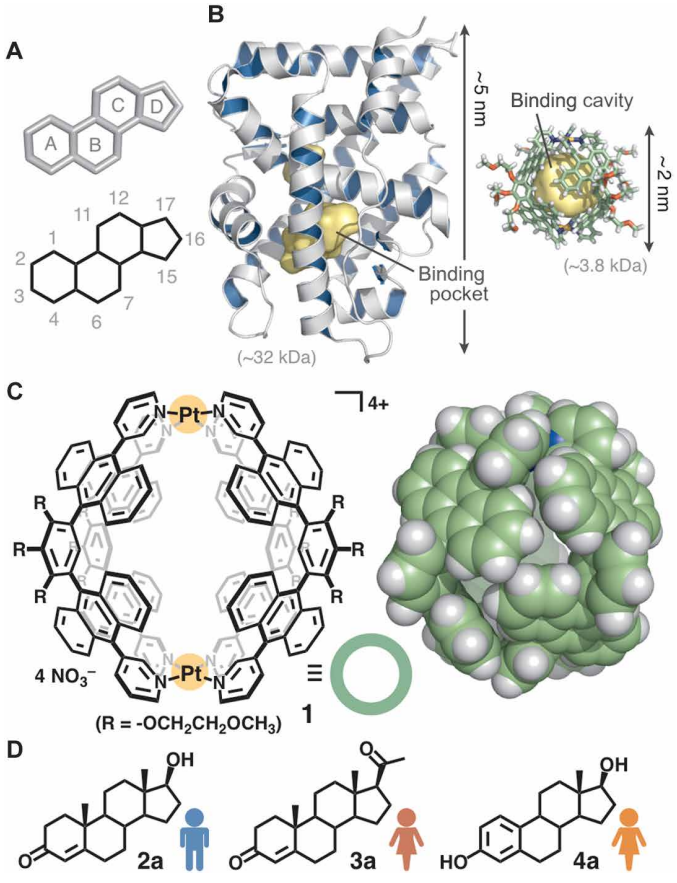

Fig. 1. Structures of steroid sex hormones, a natural androgen receptor, and a synthetic receptor. (**A**) Tetracyclic framework of steroid sex hormones. (**B**) Crystal structures of a human androgen receptor (*6*, left) and synthetic receptor **1** (right) shown at the same scale. The binding pocket and cavity are highlighted in yellow. (**C**) Polyaromatic receptor **1** used here and space-filling representation of the core framework (based on the crystal structure). (**D**) Representative male hormone, testosterone (**2a**), and female hormones, progesterone (**3a**) and β-estradiol (**4a**).

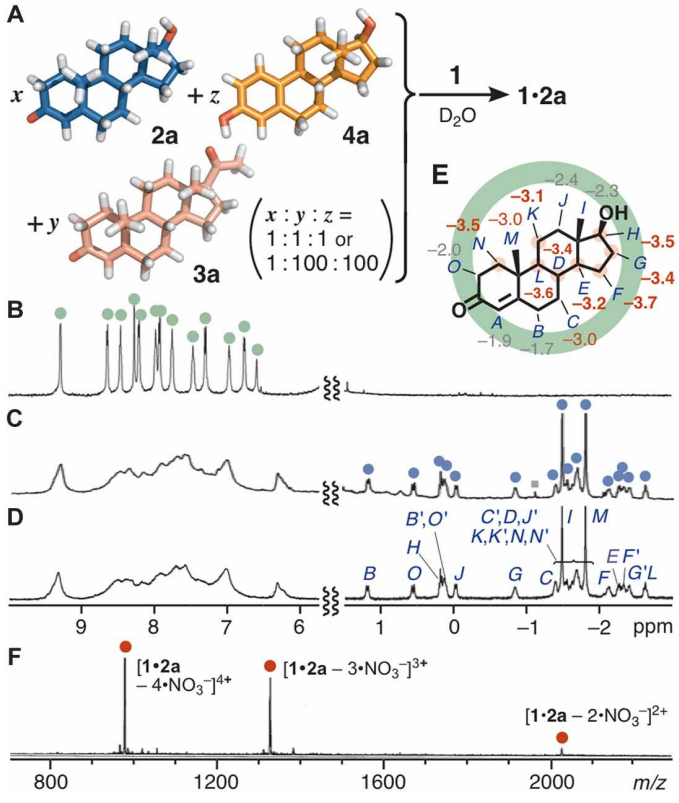

Fig. 2. Selective binding of testosterone by receptor 1 from mixtures. (**A**) Schematic representation of the selective binding of testosterone (**2a**) by receptor **1** from a mixture of **2a**, progesterone (**3a**), and β-estradiol (**4a**) (1:1:1 or 1:100:100 ratio) in water. ^{1}H NMR spectra (500 MHz, D_2O) of (**B**) receptor **1** and (**C**) products obtained from an equimolar mixture of **2a**, **3a**, and **4a** in the presence of **1** at 60°C for 10 min (gray square, **1•3a**) and (**D**) **1•2a**. (**E**) Changes of the ^{1}H NMR chemical shifts (Δδ in ppm) of **2a** upon encapsulation by **1**. (**F**) ESI-TOF MS spectrum (H_2O, room temperature) of **1•2a**.

3a and **4a** (Fig. 2D and fig. S5) and subsequently analyzed the two-dimensional (2D) NMR spectra (figs. S6 to S10) and the mass spectrometry (MS) spectrum (fig. S11). The detailed spectral analyses revealed that the sharp but complex ^{1}H NMR signals in the range of −2.62 to 1.19 parts per million (ppm) and at 3.83 ppm are assignable to the inequivalent 27 protons on **2a** in the cavity of **1**. Upon encapsulation, the methylene (H_F, H_G, H_K, and H_N) and methine (H_D, H_E, H_H, and H_L) signals for **2a** showed outstanding upfield shifts (Δδ < −3.0 ppm; Fig. 2, D and E) due to the effective aromatic shielding effect through the close proximity to the anthracene panels of **1**. The aromatic proton signals of **1•2a** were substantially broadened, as compared with free **1** (Fig. 2B), indicating the desymmetrization and restricted motion of the receptor framework through strong host-guest interactions in the cavity. The broadened host signals became sharp at 80°C (fig. S5C). The formation of complex **1•2a** was further confirmed by the electrospray ionization time-of-flight (ESI-TOF) MS spectrum, displaying a series of the prominent peaks of $[\mathbf{1{\bullet}2a} - n{\bullet}NO_3^-]^{n+}$ (n = 4 to 2) species (Fig. 2F). Although tiny proton signals (<2%) were found, e.g., at −1.13 ppm, corresponding to the signals of **1•3a**, no signals were detected from **1•4a** or free **1** (Fig. 2C and figs. S12 to S15).

The selectivity of receptor **1** toward **2a** is quite high. The receptor selectively encapsulated **2a** from a suspended aqueous solution of **2a** containing a large excess of **3a** and **4a** (100 equiv each) (Fig. 2A). The ^{1}H NMR analysis elucidated the exclusive formation of **1•2a** in >98% yield within 10 min at 60°C (fig. S2C). In this experiment, the formation of **1•3a** (68%), **1•4a** (32%), and **1•2a** (trace) was observed for 1 min at room temperature (fig. S2D). The ^{1}H NMR and MS spectra of **1•2a** displayed that the host-guest structure is stable enough in water even under high dilution conditions (<5.0 μM) (fig. S16), indicating that the binding constant (K_a) is quite high. By the competitive binding studies with a water-soluble oligo(ethylene oxide) guest, 18-crown-6, in water (*33*), the binding constant (K) of **1** toward male hormone **2a** was estimated to be 4.5×10^7 M^{-1}, which is >100 times higher than that for female hormone **3a** (fig. S17 and table S1). Both the nonclassical and classical hydrophobic effects largely contribute to the present strong binding of rigid hydrophobic substrates (*36*), on the basis of our earlier reports on the encapsulation of flexible hydrophilic substrates in water (*30*, *32*, *33*).

Detailed interactions between the receptor and testosterone

To unravel the detailed host-guest interactions between synthetic receptor **1** and male hormone **2a**, we successfully prepared high-quality,

pale yellow crystals suitable for the precise x-ray structural analysis by slow evaporation of a H_2O solution of **1'•2a** at room temperature over 1 week. Receptor **1'** is an analog of **1**, in which the Pt(II) ions and NO_3^- counterions are replaced by Pd(II) ions and BF_4^- ions, respectively. The crystal analysis data show that the relatively large steroid framework of **2a** (>1.1 nm in long-axis length and 315 $Å^3$ in volume) is fully encapsulated within the polyaromatic shell (521 $Å^3$ in cavity volume) of **1'** (Fig. 3, A and B, and fig. S18A). The packing coefficient was estimated to be 60% (table S2), indicating the importance of host-guest dispersion interactions (*37*). The spherical cavity of receptor **1** was distorted into an elliptical shape upon encapsulation. This substrate-induced conformational change (i.e., induced-fit mechanism) plays a vital role in the observed shape discrimination for rigid steroid substrates by the semirigid metal-organic receptor. In the deformed nanocavity of **1'**, the polyaromatic panels are in close contact with the edges of the tetracyclic hydrocarbon skeleton and one planar surface (without the methyl groups) of **2a** (Fig. 3C). The large upfield shifts of the proton NMR peaks of **2a** within **1** (Fig. 2E) indicate that these close contacts also exist in solution. Furthermore, three types of host-guest interactions are present in the crystal structure (Fig. 3D): (i) 10 CH-π interactions (i.e., dispersion interactions) within distances of 3.3 Å between the methylene or methine hydrogen atoms of **2a** and the host aromatic rings (*26*, *27*, *30*, *33*), (ii) two OH-π interactions within distances of 3.5 Å between the hydroxyl oxygen atom of **2a** and the host aromatic rings (*36*), and (iii) two hydrogen-bonding interactions within distances of 3.3 Å between the same oxygen atom and the acidic α-hydrogen atoms on the host pyridyl rings (*32*, *33*, *38*). These three-dimensional multiple noncovalent interactions contribute to the recognition of tiny structural differences and shapes of substrates **2a**, **3a**, and **4a**. Crystals of **1•3a** and **1•4a** proved elusive, but the optimized structures indicate the full encapsulation of the guest substrates in the polyaromatic cavity accompanied by large conformational changes (fig. S19).

Binding affinity of the receptor toward male hormones

The binding affinity of receptor **1** toward male hormones **2a**, dehydroepiandrosterone (**2b**), dihydrotestosterone (**2c**), androstenedione (**2d**), and androsterone (**2e**) was established through competitive encapsulation experiments under the similar conditions as above (Fig. 4A). For example, the treatment of **2a** and **2c** (1.0 equiv each) with **1** gave rise to host-guest complexes **1•2a** and **1•2c** in a 51:49 ratio (fig. S20). The only structural difference between **2a** and **2c** is the presence (and absence) of a double bond on the A ring. The methyl peaks for both **2a** and **2c** within **1** were observed at −1.5 to 2.0 ppm in the ^1H NMR spectrum (Fig. 4B, bottom). Receptor **1** preferentially bound **2a** from a mixture of **2a** and **2d** to give complexes **1•2a** and **1•2d** in a 61:39 ratio (Fig. 4C and fig. S21). Hormones **2a** and **2d** differ by a single functional group, a hydroxy or carbonyl group, at the 17-position. Further competitive studies established the binding affinities of **1** for the male hormones to be **2b** ≈ **2a** ≈ **2c** > **2d** > **2e** (figs. S22 to S24 and S37 to S40). Whereas the water solubility of the tested hormones is different (table S3) (*10*, *39*), the observed order stems from not the solubility but the affinity of the substrates toward the receptor cavity in water. The low binding affinity of **1** for **2e** likely arises from the steric repulsion between the axial 3-hydroxy group and the panels.

Next, the binding of synthetic and non-sex hormones was examined. Synthetic receptor **1** bound methyltestosterone (**5a**), a synthetic testosterone analog known as an anabolic steroid (*40*), stronger than **2a** in water (in an 83:17 ratio; Fig. 4D and figs. S25 and S45). The native androgen receptor shows the opposite binding trend (*7*). The methyl group of **5a** at the 17α-position leads to greater hydrophobic CH-polyaromatic interactions within **1**. The receptor selectively bound androstenedione (**2d**) over adrenosterone (**5b**), which is an androgenic hormone occurring primarily in fish (Fig. 4E and figs. S26 and S46) (*41*). The minor difference in the functional group (i.e., a methyl group on **5a** and a carbonyl group on **5b**) was definitively recognized by synthetic receptor **1**.

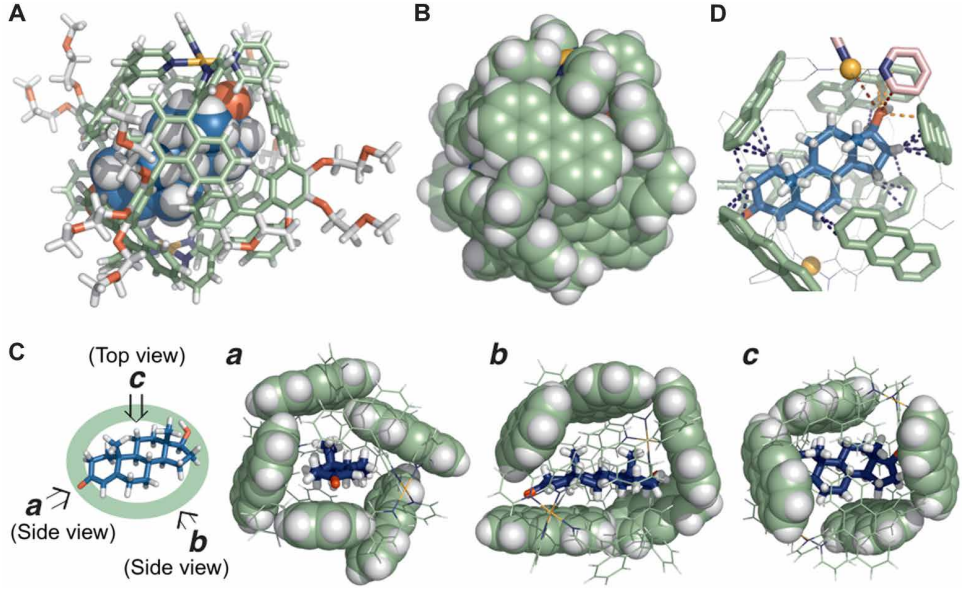

Fig. 3. X-ray crystal structure of 1'•2a. (**A**) Space-filling (for **2a**) and cylindrical (for **1'**) representation and (**B**) space-filling representation (the peripheral substituents of **1'** are replaced by hydrogen atoms for clarity). (**C**) Highlighted positions of **2a** inside the polyaromatic shell of **1'** (three different views). (**D**) Highlighted host-guest interactions of **1'•2a** in the cavity (blue, orange, and red dashed lines are CH-π, OH-π, and hydrogen-bonding interactions, respectively).

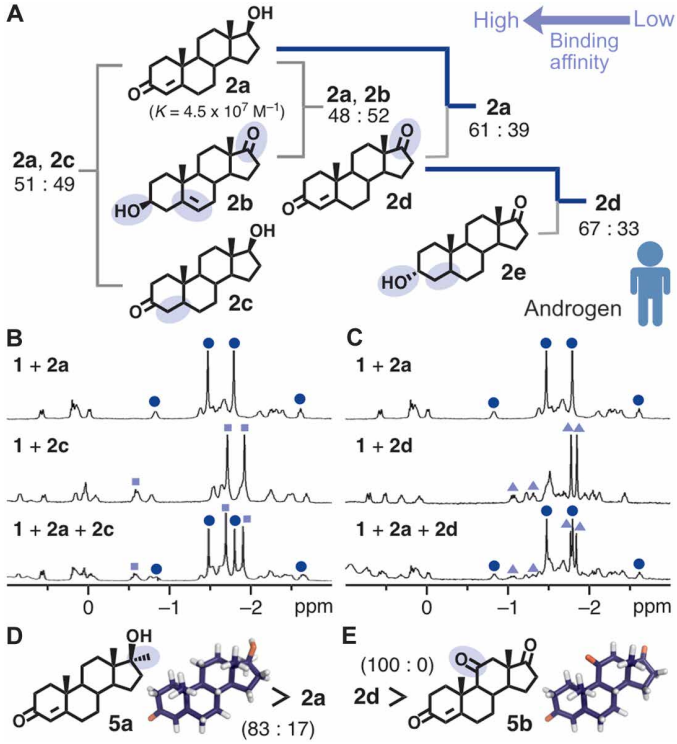

Fig. 4. Binding affinity of receptor 1 toward male hormones. (**A**) Schematic representation of the binding preference of receptor **1** toward male hormones **2a** to **2e** in water. (**B**) ^{1}H NMR spectra (500 MHz, D_2O, room temperature) of **1•2a** (top), **1•2c** (middle), and the product (bottom) obtained from an equimolar mixture of **2a** and **2c** with **1** (blue circle, **1•2a**; pale blue square, **1•2c**). (**C**) ^{1}H NMR spectra (500 MHz, D_2O, room temperature) of **1•2a** (top), **1•2d** (middle), and the product (bottom) obtained from an equimolar mixture of **2a** and **2d** with **1** (blue circle, **1•2a**; pale blue triangle, **1•2d**). Binding preference of **1** toward (**D**) **2a** and methyltestosterone (**5a**) and (**E**) **2d** and adrenosterone (**5b**) in water.

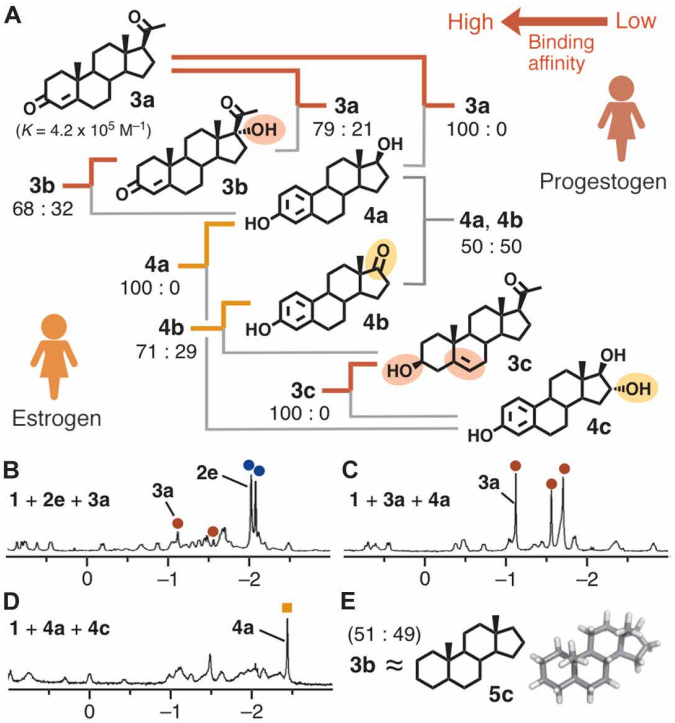

Fig. 5. Binding affinity of receptor 1 toward female hormones. (**A**) Schematic representation of the binding preference of receptor **1** toward female hormones **3a** to **3c** and **4a** to **4c** in water. ^{1}H NMR spectra (500 MHz, D_2O, room temperature) of products obtained from equimolar mixtures of (**B**) **2e** and **3a**, (**C**) **3a** and **4a**, and (**D**) **4a** and **4c** with **1**. (**E**) Binding preference of **1** toward **3b** and 5α-androstane (**5c**) in water.

Binding affinity of the receptor toward female hormones

Female hormones **3a**, 17α-hydroxyprogesterone (**3b**), and pregnenolone (**3c**), known as progestogen, as well as **4a**, estrone (**4b**), and estriol (**4c**), known as estrogen (Fig. 5A), were preferentially bound by receptor **1** in the following order: **3a** > **3b** > **4a** ≈ **4b** > **3c** > **4c** (figs. S27 to S34 and S41 to S44). The strongest bound female hormone studied here, **3a** ($K = 4.2 \times 10^5$ M^{-1}), was still weakly encapsulated by **1** (in a 14:86 ratio) from a 1:1 mixture of **3a** and male hormone **2e** (Fig. 5B and fig. S27). Whereas the core frameworks of **3a** and **2a** are the same, the steric difference between the acetyl and hydroxy groups drastically alters their binding affinities to the receptor (fig. S3). The bulky acetyl group at the 17β-position prevents effective encapsulation of all progestogenic hormones **3a** to **3c** by **1**. Surprisingly, receptor **1** exclusively bound progestogen **3a** from an equimolar mixture of **3a** and estrogen **4a** in water (Fig. 5C and fig. S28). The aromatic A ring in estrogenic hormones **4a** to **4c** rigidifies the steroid backbone and definitely weakens their bindings toward **1**. As an exception, the binding of progestogen **3c** is weaker than that of estrogens **4a** and **4b** due to the sterically hindered 17β-acetyl and hydrophilic 3β-hydroxy groups (fig. S32). Receptor **1** exclusively bound **4a** from a mixture of **4a** and **4c**, recognizing the extra 16-hydroxy group (Fig. 5D and fig. S34).

The parent hydrocarbon skeleton of male and female hormones, 5α-androstane (**5c**), was also encapsulated by receptor **1** with an affinity comparable to that of **3b** (Fig. 5E and figs. S35 and S47). Crystals of host-guest complex **1"•5c** were obtained using analogous Pd(II)-linked receptor **1"** with NO_3^- counterions. The crystal structure analysis again confirmed the existence of multiple close contacts (≤3.2 Å) between the guest hydrocarbon and the polyaromatic panels of receptor **1"** (fig. S18, B to D).

Unlike natural androgen receptors with protein pockets containing multiple hydrogen-bonding sites (*6*, *7*), receptor **1** provides a relatively simple hydrophobic cavity defined by the polyaromatic panels (Fig. 1C). The artificial cavity is rigid yet flexible enough to deform to complement the guest shape and enhance host-guest interactions (i.e., CH/OH-π and hydrogen-bonding contacts; Fig. 3D), which is fully different from the cavity properties of previously reported cage-shaped and tubular receptors (*9*–*21*). This shape-complementary enveloping of the hormone frameworks is highly sensitive to changes of key functional groups on their terminal A and D rings, where the best fit is accomplished by the male hormones. The substrate-induced conformational changes are necessary to effect specific substrate-receptor interactions in the cavity and thereby establish the thermodynamic stabilities of the resultant host-guest complexes in water.

Fluorescent detection of testosterone by a receptor-dye complex

Last, as an initial step for the development of ultrasensitive analytical devices based on single-molecule detection, we set up a prototypical detection system for male hormones based on the displacement of a fluorescent dye within the synthetic receptor. Bound within receptor

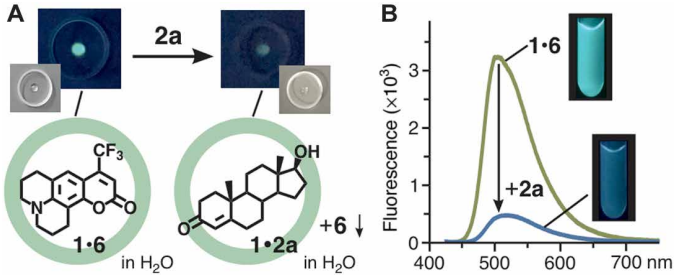

Fig. 6. Fluorescent detection of testosterone by receptor-dye complex 1•6. (**A**) Schematic representation of nanogram-scale fluorescent detection of male hormone **2a** using one drop of an aqueous **1•6** solution (8 μM) and their photographs (λ_{ex} = 356 nm) on a petri dish. (**B**) Fluorescence spectra (room temperature, λ_{ex} = 423 nm) of a H_2O solution of **1•6** (78 μM, 0.5 ml) before and after addition of **2a** (45 nmol) and their photographs (λ_{ex} = 356 nm).

1, hydrophobic coumarin 153 (**6**) emits bluish green fluorescence (λ_{max} = 509 nm, Φ_F = 25%) in water upon excitation at 423 nm (Fig. 6A) (*42*). The emission of **1•6** decreases as the dye guest is displaced by a more hydrophobic hormone guest in water (fig. S48). When one drop (100 μl) of an H_2O solution of **1•6** (8 μM) was added to a nanogram amount of **2a** (230 ng, 0.80 nmol), the bluish green emission was markedly weakened after brief sonication (20 s) at room temperature (Fig. 6A). The displaced dye **6** is non-emissive due to the formation of aggregated precipitates. Accordingly, the visual detection of infinitesimal testosterone could be carried out on a small petri dish. In fluorescence spectra, the emission intensity of **1•6** (78 μM, 0.5 ml) in water largely decreased (−85%) upon addition of **2a** (45 nmol) at room temperature within 10 min (Fig. 6B).

DISCUSSION

We have realized the discrimination between steroid male and female hormones by a synthetic molecular receptor in water. The binding affinity resembles that of natural androgen receptors: Androgenic male hormones are predominantly encapsulated by the receptor even from mixtures including large excess progestogenic and estrogenic female hormones. The key of the present achievement is using a semi-rigid nanocavity surrounded by polyaromatic frameworks linked by metal ions, which can deform the shape to enhance interactions between the substrates and cavity. The combination of the polyaromatic receptor with high androgen affinity and advanced analytical methods based on single-molecule detection (*1*–*3*) would develop novel ultrasensitive analytical devices for steroid sex hormones, one of the most important and complex biosubstrates with high physiological activities.

MATERIALS AND METHODS

Chemicals

Receptor **1** (*28*) and a host-guest complex containing coumarin 153 (*42*) were synthesized according to previously reported procedures. Solvents and reagents were purchased from the following commercial suppliers: TCI Co. Ltd., Wako Pure Chemical Industries Ltd., Kanto Chemical Co. Inc., Sigma-Aldrich Co., and Cambridge Isotope Laboratories Inc.

General

The following analytical instruments were used: NMR, Bruker ASCEND-500 (500 MHz); ESI-TOF MS, Bruker micrOTOF II; Fourier transform infrared (FTIR), JASCO FT/IR-4200; ultraviolet-visible spectrophotometry, JASCO V-670DS; fluorescence, HITACHI F-7000; x-ray, Bruker APEXII ULTRA/CCD and AXS D8 VENTURE/PHOTON 100 diffractometers; calculation, Materials Studio (version 5.5.3; Accelrys Software Inc.) and SCIGRESS program (version FJ 2.6; Fujitsu Ltd., Japan).

Competitive binding experiments of 2a, 3a, and 4a with 1

Receptor **1** (1.5 mg, 0.39 μmol), testosterone (**2a**; 0.1 mg, 0.39 μmol), progesterone (**3a**; 0.1 mg, 0.39 μmol), β-estradiol (**4a**; 0.1 mg, 0.39 μmol), and D_2O (0.5 ml) were added to a glass test tube. The mixture was stirred at 60°C for 10 min. The selective formation of a **1•2a** complex was confirmed in ~98% yield by ^{1}H NMR analysis. The selective formation of a **1•2a** complex was observed even from **1** and a mixture of **2a** (1 equiv) and **3a** and **4a** (100 equiv each) under the same conditions. When the complex mixture was stirred at room temperature for 1 min, the formation of **1•2a** (trace), **1•3a** (68%), and **1•4a** (32%) was observed in the ^{1}H NMR spectrum.

Structural characterization of 1•2a

Receptor **1** (1.5 mg, 0.39 μmol), testosterone (**2a**; 0.1 mg, 0.39 μmol), and D_2O (0.5 ml) were added to a glass test tube (2.0 ml). The mixture was stirred at 60°C for 10 min. The quantitative formation of a **1•2a** complex was confirmed by NMR and ESI-TOF MS analyses. The encapsulation experiments of **2b** to **2e**, **3a** to **3c**, **4a** to **4c**, and **5a** to **5c** (0.39 μmol each) by **1** (1.5 mg, 0.39 μmol) were examined under the same conditions.

^{1}H NMR (500 MHz, D_2O, room temperature): δ −2.63 (t, *J* = 11.5 Hz, **2a**), −2.41 (m, **2a**), −2.33 (m, **2a**), −2.27 (m, **2a**), −2.13 (m, **2a**), −1.81 (s, **2a**), −1.77 to −1.51 (m, **2a**), −1.49 (s, **2a**), −1.39 (m, **2a**), −0.84 (m, **2a**), −0.03 (d, *J* = 10.5 Hz, **2a**), 0.06 to 0.24 (m, **2a**), 0.56 (d, *J* = 15.0 Hz, **2a**), 1.19 (d, *J* = 13.0 Hz, **2a**), 2.46 (br, 24H, **1**), 3.00 (br, 16H, **1**), 3.47 (s, 12H, **1**), 3.83 (s, **2a**), 3.93 (m, 8H, **1**), 4.04 (m, 16H, **1**), 4.46 (m, 4H, **1**), 4.64 (m, 4H, **1**), 6.33 (br, 4H, **1**), 7.02 (br, **1**), 7.42 (br, **1**), 7.59 (br, **1**), 7.71 (br, **1**), 7.93 (br, **1**), 8.18 (br, **1**), 8.39 (br, **1**), 8.51 (br, **1**), 9.32 (br, 8H, **1**). ^{1}H NMR (500 MHz, D_2O, 80°C): δ −2.61 (m, **2a**), −2.36 (m, **2a**), −2.31 to −2.17 (m, **2a**), −2.08 (m, **2a**), −1.87 to −1.60 (m, **2a**), −1.82 (s, **2a**), −1.48 (m, **2a**), −1.46 (m, **2a**), −1.40 (s, **2a**), −1.36 (m, **2a**), −0.86 (m, **2a**), −0.05 (d, *J* = 12.0 Hz, **2a**), −0.01 to 0.16 (m, **2a**), 0.22 (t, *J* = 8.5 Hz, **2a**), 0.41 (d, *J* = 16.0 Hz, **2a**), 1.12 (d, *J* = 13.0 Hz, **2a**), 2.48 (s, 24H, **1**), 3.04 (m, 8H, **1**), 3.09 (m, 8H, **1**), 3.48 (s, 12H, **1**), 3.83 (s, **2a**), 3.88 (m, 8H, **1**), 3.94 (t, *J* = 4.5 Hz, 8H, **1**), 4.04 (m, 8H, **1**), 4.49 (m, 4H, **1**), 4.64 (m, 4H, **1**), 6.16 to 6.55 (br, 16H, **1**), 6.25 (s, 4H, **1**), 6.78 (br, 8H, **1**), 7.02 (d, *J* = 8.0 Hz, 8H, **1**), 7.50 (dd, *J* = 5.5, 8.0 Hz, 8H, **1**), 7.67 (m, 16H, **1**), 7.89 (s, 8H, **1**), 7.98 (d, *J* = 8.0 Hz, 8H, **1**), 8.42 (dd, *J* = 5.5, 7.5 Hz, 8H, **1**), 8.58 (d, *J* = 7.5 Hz, 8H, **1**), 9.33 (d, *J* = 5.5 Hz, 8H, **1**). FTIR (KBr, cm^{-1}): 3407, 3061, 2928, 2883, 2833, 1955, 1638, 1520, 1384, 1100, 1065, 1028, 944, 824, 769, 705, 644. ESI-TOF MS (H_2O): *m*/*z* 2014.9 [**1•2a** − $2NO_3^-$]$^{2+}$, 1322.6 [**1•2a** − $3NO_3^-$]$^{3+}$, 976.4 [**1•2a** − $4NO_3^-$]$^{4+}$.

Binding constants of 1 toward 2a and 3a

The binding constants (*K*) of **1** toward **2a** and **3a** were determined by the competitive binding experiments with water-soluble 18-crown-6 (**CE**). On the basis of the *K* value of **CE** toward **1** (2.3×10^6 M^{-1}) (*33*), the binding constant for **2a** was estimated using the ^{1}H NMR integral ratios of **1•2a** and **1•CE**. For example, **CE** (51 μg, 0.19 μmol) was added to a D_2O (0.5 ml) solution of water-soluble **1•2a** (0.8 mg, 0.19 μmol). After the 1:1 mixture was stirred at 60°C for 3 hours, the

concentration of the resultant host-guest complexes was determined on the basis of the ^{1}H NMR spectrum (fig. S17). The concentration of the released **2a** from **1** was calculated to be 0.072 mM from $[\mathbf{1}\bullet\mathbf{2a}]_{initial} - [\mathbf{1}\bullet\mathbf{2a}]_{final}$ because of the complex ^{1}H NMR signals and low solubility of **2a**. The value is comparable to the reported solubility of **2a** in water (~0.1 mM at room temperature). By the similar experiments under various host-guest ratios (1:0.5, 1:2, 1:2.5, and/or 1:4 ratios; fig. S17 and table S1), the binding constants of **1** toward **2a** and **3a** were estimated to be at least 4.5×10^7 and 4.2×10^5 M^{-1}, respectively.

Competitive binding experiment of 2a and 3a with 1

Receptor **1** (1.5 mg, 0.39 μmol), testosterone (**2a**; 0.1 mg, 0.39 μmol), progesterone (**3a**; 0.1 mg, 0.39 μmol), and D_2O (0.5 ml) were added to a glass test tube. The mixture was stirred at 60°C for 10 min. The formation and ratio of **1•2a** and **1•3a** complexes were confirmed by ^{1}H NMR analysis (fig. S3). Similarly, the competitive binding experiments of **2a** and **4a** (fig. S4), **2a** and **2c** (fig. S20), **2a** and **2d** (fig. S21), **2a** and **2b** (fig. S22), **2b** and **2c** (fig. S23), **2d** and **2e** (fig. S24), **2a** and **5a** (fig. S25), **2d** and **5b** (fig. S26), **2e** and **3a** (fig. S27), **3a** and **4a** (fig. S28), **3a** and **3b** (fig. S29), **3b** and **4a** (fig. S30), **4a** and **4b** (fig. S31), **3c** and **4a** (fig. S32), **3c** and **4c** (fig. S33), **4a** and **4c** (fig. S34), **3b** and **5c** (fig. S35), and **4a** and **5c** (fig. S36) were examined using **1** in water.

Fluorescent detection of male hormone 2a

One drop (100 μl) of a H_2O solution of **1•6** (8 μM) was added to male hormone **2a** (230 ng, 0.80 nmol) at room temperature. After brief sonication (20 s) and standing in the dark (3 min) at room temperature, the bluish green emission was markedly weakened. Similarly, hormone **2a** (13 μg, 45 nmol) was suspended in a D_2O solution of **1•6** (78 μM, 0.5 ml) at room temperature for 10 min. The resultant mixture was filtered and then confirmed by ^{1}H NMR and fluorescence analyses.

X-ray crystal data of 1'•2a and 1"•5c

CCDC-1539560 and CCDC-1485686 contain the supplementary crystallographic data (tables S4 and S5) for the structures reported in this article. These data can be obtained free of charge from The Cambridge Crystallographic Data Centre (CCDC) via www.ccdc.cam.ac.uk/data_request/cif.

SUPPLEMENTARY MATERIALS

Supplementary material for this article is available at http://advances.sciencemag.org/cgi/content/full/5/4/eaav3179/DC1

REFERENCES AND NOTES

1. A. P. de Silva, H. Q. N. Gunaratne, T. Gunnlaugsson, A. J. M. Huxley, C. P. McCoy, J. T. Rademacher, T. E. Rice, Signaling recognition events with fluorescent sensors and switches. *Chem. Rev.* **97**, 1515–1566 (1997).
2. J. Janata, M. Josowicz, P. Vanýsek, D. M. DeVaney, Chemical sensors. *Anal. Chem.* **70**, 179–208 (1998).
3. B. Wang, E. V. Anslyn, *Chemosensors: Principles, Strategies, and Applications* (Wiley, 2011).
4. W. L. Miller, Molecular biology of steroid hormone synthesis. *Endocr. Rev.* **9**, 295–318 (1988).
5. A. W. Norman, M. T. Mizwicki, D. P. G. Norman, Steroid-hormone rapid actions, membrane receptors and a conformational ensemble model. *Nat. Rev. Drug Discov.* **3**, 27–41 (2004).
6. K. Pereira de Jésus-Tran, P.-L. Côté, L. Cantin, J. Blanchet, F. Labrie, R. Breton, Comparison of crystal structures of human androgen receptor ligand-binding domain complexed with various agonists reveals molecular determinants responsible for binding affinity. *Protein Sci.* **15**, 987–999 (2006).
7. W. Gao, C. E. Bohl, J. T. Dalton, Chemistry and structural biology of androgen receptor. *Chem. Rev.* **105**, 3352–3370 (2005).
8. H. Fang, W. Tong, W. S. Branham, C. L. Moland, S. L. Dial, H. Hong, Q. Xie, R. Perkins, W. Owens, D. M. Sheehan, Study of 202 natural, synthetic, and environmental chemicals for binding to the androgen receptor. *Chem. Res. Toxicol.* **16**, 1338–1358 (2003).
9. K. Uekama, T. Fujinaga, F. Hirayama, M. Otagiri, M. Yamasaki, Inclusion complexations of steroid hormones with cyclodextrins in water and in solid phase. *Int. J. Pharm.* **10**, 1–15 (1982).
10. A. I. Lazar, F. Biedermann, K. R. Mustafina, K. I. Assaf, A. Hennig, W. M. Nau, Nanomolar binding of steroids to cucurbit[*n*]urils: Selectivity and applications. *J. Am. Chem. Soc.* **138**, 13022–13029 (2016).
11. A. Stahl, A. I. Lazar, V. N. Muchemu, W. M. Nau, M. S. Ullrich, A. Hennig, A fluorescent, supramolecular chemosensor to follow steroid depletion in bacterial cultures. *Anal. Bioanal. Chem.* **409**, 6485–6494 (2017).
12. S. Kumar, H.-J. Schneider, The complexation of estrogens and tetralins in the cavities of azoniacyclophanes. A ^{1}H and ^{13}C nuclear magnetic resonance spectroscopic study. *J. Chem. Soc. Perkin Trans.* **2**, 245–250 (1989).

13. T. Marti, B. R. Peterson, A. Fürer, T. Mordasini-Denti, J. Zarske, B. Jaun, F. Diederich, V. Gramlich, Macrotricyclic steroid receptors by Pd°-catalyzed cross-coupling reactions: Dissolution of cholesterol in aqueous solution and investigations of the principles governing selective molecular recognition of steroidal substrates. *Helv. Chim. Acta* **81**, 109–144 (1998).
14. I. Higler, P. Timmerman, W. Verboom, D. N. Reinhoudt, Combination of calix[4]arenes and resorcin[4]arenes for the complexation of steroids. *J. Org. Chem.* **61**, 5920–5931 (1996).
15. M. Cacciarini, V. A. Azov, P. Seiler, H. Künzerc, F. Diederich, Selective steroid recognition by a partially bridged resorcin[4]arene cavitand. *Chem. Commun.*, 5269–5271 (2005).
16. K. Srinivasan, B. C. Gibb, Synthesis of nanoscale carceplexes from deep-cavity cavitands. *Chem. Commun.*, 4640–4642 (2008).
17. S. C. Hong, D. P. Murale, M. Lee, S. M. Lee, J. S. Park, J.-S. Lee, Bulk aggregation based fluorescence turn-on sensors for selective detection of progesterone in aqueous solution. *Angew. Chem. Int. Ed.* **56**, 14642–14647 (2017).
18. C. L. D. Gibb, B. C. Gibb, Well-defined, organic nanoenvironments in water: The hydrophobic effect drives a capsular assembly. *J. Am. Chem. Soc.* **126**, 11408–11409 (2004).
19. T. K. Ronson, A. B. League, L. Gagliardi, C. J. Cramer, J. R. Nitschke, Pyrene-edged $Fe^{II}_4L_6$ cages adaptively reconfigure during guest binding. *J. Am. Chem. Soc.* **136**, 15615–15624 (2014).
20. E. G. Percástegui, J. Mosquera, J. R. Nitschke, Anion exchange renders hydrophobic capsules and cargoes water-soluble. *Angew. Chem. Int. Ed.* **56**, 9136–9140 (2017).
21. J. Mendez-Arroyo, A. I. d'Aquino, A. B. Chinen, Y. D. Manraj, C. A. Mirkin, Reversible and selective encapsulation of dextromethorphan and β-estradiol using an asymmetric molecular capsule assembled via the weak-link approach. *J. Am. Chem. Soc.* **139**, 1368–1371 (2017).
22. P. Willimann, T. Marti, A. Fürer, F. Diederich, Steroids in molecular recognition. *Chem. Rev.* **97**, 1567–1608 (1997).
23. H.-J. Schneider, P. Agrawal, A. K. Yatsimirsky, Supramolecular complexations of natural products. *Chem. Soc. Rev.* **42**, 6777–6800 (2013).
24. N. Kishi, Z. Li, K. Yoza, M. Akita, M. Yoshizawa, An M_2L_4 molecular capsule with an anthracene shell: Encapsulation of large guests up to 1 nm. *J. Am. Chem. Soc.* **133**, 11438–11441 (2011).
25. C. A. Hunter, K. R. Lawson, J. Perkins, C. J. Urch, Aromatic interactions. *J. Chem. Soc. Perkin Trans. 2*, 651–669 (2001).
26. M. Nishio, The CH/π hydrogen bond in chemistry. Conformation, supramolecules, optical resolution and interactions involving carbohydrates. *Phys. Chem. Chem. Phys.* **13**, 13873–13900 (2011).
27. K. Yazaki, Y. Sei, M. Akita, M. Yoshizawa, A polyaromatic molecular tube that binds long hydrocarbons with high selectivity. *Nat. Commun.* **5**, 5179 (2014).
28. M. Yamashina, Y. Sei, M. Akita, M. Yoshizawa, Safe storage of radical initiators within a polyaromatic nanocapsule. *Nat. Commun.* **5**, 4662 (2014).
29. A. Ahmedova, D. Momekova, M. Yamashina, P. Shestakova, G. Momekov, M. Akita, M. Yoshizawa, Anticancer potencies of Pt^{II}- and Pd^{II}-linked M_2L_4 coordination capsules with improved selectivity. *Chem. Asian J.* **11**, 474–477 (2016).
30. M. Yamashina, M. Akita, T. Hasegawa, S. Hayashi, M. Yoshizawa, A polyaromatic nanocapsule as a sucrose receptor in water. *Sci. Adv.* **3**, e1701126 (2017).
31. S. Matsuno, M. Yamashina, Y. Sei, M. Akita, A. Kuzume, K. Yamamoto, M. Yoshizawa, Exact mass analysis of sulfur clusters upon encapsulation by a polyaromatic capsular matrix. *Nat. Commun.* **8**, 749 (2017).
32. S. Kusaba, M. Yamashina, M. Akita, T. Kikuchi, M. Yoshizawa, Hydrophilic oligo(lactic acid)s captured by a hydrophobic polyaromatic cavity in water. *Angew. Chem. Int. Ed.* **57**, 3706–3710 (2018).
33. M. Yamashina, S. Kusaba, M. Akita, T. Kikuchi, M. Yoshizawa, Cramming versus threading of long amphiphilic oligomers into a polyaromatic capsule. *Nat. Commun.* **9**, 4227 (2018).
34. M. Yoshizawa, J. K. Klosterman, Molecular architectures of multi-anthracene assemblies. *Chem. Soc. Rev.* **43**, 1885–1898 (2014).
35. M. Yoshizawa, M. Yamashina, Coordination-driven nanostructures with polyaromatic shells. *Chem. Lett.* **46**, 163–171 (2017).
36. E. A. Meyer, R. K. Castellano, F. Diederich, Interactions with aromatic rings in chemical and biological recognition. *Angew. Chem. Int. Ed.* **42**, 1210–1250 (2003).
37. S. Mecozzi, J. Rebek Jr., The 55% solution: A formula for molecular recognition in the liquid state. *Chem. A Eur. J.* **4**, 1016–1022 (1998).
38. D. P. August, G. S. Nichol, P. J. Lusby, Maximizing coordination capsule–guest polar interactions in apolar solvents reveals significant binding. *Angew. Chem. Int. Ed.* **55**, 15022–15026 (2016).
39. S. H. Yalkowsky, Y. He, P. Jain, *Handbook of Aqueous Solubility Data* (CRC Press, ed. 2, 2010).
40. H. A. Haupt, G. D. Rovere, Anabolic steroids: A review of the literature. *Am. J. Sports Med.* **12**, 469–484 (1984).
41. D. R. Idler, I. I. Bitners, P. J. Schmidt, 11-Ketotestosterone: An androgen for sockeye salmon. *Can. J. Biochem. Physiol.* **39**, 1737–1742 (1961).
42. M. Yamashina, M. M. Sartin, Y. Sei, M. Akita, S. Takeuchi, T. Tahara, M. Yoshizawa, Preparation of highly fluorescent host–guest complexes with tunable color upon encapsulation. *J. Am. Chem. Soc.* **137**, 9266–9269 (2015).

Acknowledgments: M.Ya. thanks the Japan Society for the Promotion of Science (JSPS) for an Overseas Research Fellowship. **Funding:** This study was supported by JSPS KAKENHI (grant numbers JP17H05359/JP18H01990) and Support for Tokyotech Advanced Researchers (STAR).
Author contributions: M.Ya. and M.Yo. designed the work, carried out research, analyzed data, and wrote the paper. T.T. analyzed experimental data. Y.S. contributed to x-ray crystallographic analysis. M.Yo. is the principal investigator. M.A. was involved in the work discussion. All authors discussed the results and commented on the manuscript. M.Yo. claims responsibility for all figures in the main text and the Supplementary Materials. **Competing interests:** The authors declare that they have no competing interests. **Data and materials availability:** All data needed to evaluate the conclusions in the paper are present in the paper and/or the Supplementary Materials. Additional data related to this paper may be requested from the authors.

Submitted 5 September 2018
Accepted 25 February 2019
Published 19 April 2019
10.1126/sciadv.aav3179

Citation: M. Yamashina, T. Tsutsui, Y. Sei, M. Akita, M. Yoshizawa, A polyaromatic receptor with high androgen affinity. *Sci. Adv.* **5**, eaav3179 (2019).

Science Advances

A polyaromatic receptor with high androgen affinity

Masahiro Yamashina, Takahiro Tsutsui, Yoshihisa Sei, Munetaka Akita and Michito Yoshizawa

Sci Adv **5** (4), eaav3179.
DOI: 10.1126/sciadv.aav3179